NeuroImage 86 (2014) 514–524

Contents lists available at ScienceDirect

NeuroImage

journal homepage: www.elsevier.com/locate/ynimg

The extrastriate body area is involved in illusory limb ownership

Jakub Limanowski [a,*], Antoine Lutti [b], Felix Blankenburg [a,c,d]

[a] Berlin School of Mind and Brain, Humboldt-Universität zu Berlin, 10117 Berlin, Germany
[b] LREN, Departement des neurosciences cliniques, CHUV, University Lausanne, Switzerland
[c] Dahlem Institute for Neuroimaging of Emotion, Freie Universität Berlin, 14195 Berlin, Germany
[d] Center for Adaptive Rationality (ARC), Max Planck Institute for Human Development, 14195 Berlin, Germany

ARTICLE INFO

Article history:
Accepted 22 October 2013
Available online 31 October 2013

Keywords:
Body ownership
Rubber Hand Illusion
fMRI
Extrastriate body area
Anterior insula

ABSTRACT

The Rubber Hand Illusion (RHI) is an established paradigm for studying body ownership, and several studies have implicated premotor and temporo-parietal brain regions in its neuronal foundation. Here we used an automated setup to induce a novel multi-site version of the RHI in healthy human participants inside an MR-scanner, with a RHI and control condition that were matched in terms of synchrony of visual and tactile stimulation. Importantly, as previous research has shown that most of the ownership-related brain areas also respond to observed human actions and touch, or body parts of others, here such potential effects of the experimenter were eliminated by the automated procedure. The RHI condition induced a strong ownership illusion; we found correspondingly stronger brain activity during the RHI versus control condition in contralateral middle occipital gyrus (mOCG) and bilateral anterior insula, which have previously been related to illusory body ownership. Using independent functional localizers, we confirmed that the activity in mOCG was located within the body-part selective extrastriate body area (EBA). Crucially, activity differences in participants' peak voxels within the left EBA correlated strongly positively with their behavioral illusion scores. Thus EBA activity also reflected interindividual differences in the experienced intensity of illusory limb ownership. Moreover, psychophysiological interaction analyses (PPI) revealed that contralateral primary somatosensory cortex had stronger brain connectivity with EBA during the RHI versus control condition, while EBA was more strongly interacting with temporo-parietal multisensory regions. In sum, our findings demonstrate a direct involvement of EBA in limb ownership.
© 2013 Elsevier Inc. All rights reserved.

Introduction

To be oneself among others, one needs to identify with a particular body (Blanke and Metzinger, 2009; Gallagher, 2000; Jeannerod, 2007). Most accounts of body ownership have emphasized multimodal information integration in hierarchical cortical networks as a fundamental mechanism underlying a coherent self-representation (Apps and Tsakiris, 2013; Blanke, 2012; Hohwy, 2007, 2010; Petkova et al., 2011; Seth et al., 2011; Tsakiris, 2010). These theories are supported by recent neuroimaging experiments that have provided novel insights into how the brain self-attributes body parts based on such integration of visual, tactile, and proprioceptive information. In the Rubber Hand Illusion (RHI; Botvinick and Cohen, 1998), synchronous stroking of a dummy body part together with one's own corresponding body part typically misleads the brain to self-attribute the dummy limb (Botvinick and Cohen, 1998; Ehrsson et al., 2004; Tsakiris and Haggard, 2005) or even a whole body (Ehrsson, 2007; Lenggenhager et al., 2007). The experience of (illusory) body ownership has been linked to activity in frontal brain regions, predominantly the ventral premotor cortex (PMv; Ehrsson et al., 2004, 2005; Petkova et al., 2011), but also posterior regions like the right temporo-parietal junction (rTPJ; Blanke et al., 2002, 2005; Ionta et al., 2011; Tsakiris et al., 2008), posterior parietal cortex and intraparietal sulcus (PPC/IPS; Brozzoli et al., 2012; Ehrsson et al., 2004; Gentile et al., 2011; Petkova et al., 2011; Shimada et al., 2005; Tsakiris, 2010), and occipito-temporal regions like the body part-selective extrastriate body area (EBA; Arzy et al., 2006; Blanke and Mohr, 2005; Downing et al., 2001; Ionta et al., 2011). Primary somatosensory cortex (SI; Kanayama et al., 2007, 2009; Lenggenhager et al., 2011; Tsakiris et al., 2007) and the anterior insula (AI; Ehrsson et al., 2007) have also been associated with body ownership. Activity in these regions has been interpreted as reflecting the degree of illusory self-attribution or "incorporation" of the fake limb or body (Blanke, 2012; Ehrsson et al., 2004; Holmes and Spence, 2004; Petkova et al., 2011; Tsakiris, 2010).

Here, we used a fully automated setup to induce a novel, multi-site version of the RHI inside an fMRI scanner with high spatial resolution, addressing two potential caveats of the procedures typically used to evoke the illusion. First, we matched visual and tactile stimuli of both RHI and control condition in temporal synchrony, in contrast to the typically used asynchronous stroking control condition where observed touch on the dummy hand and felt touch on the own hand are presented serially. In our control condition, observed and felt touch were presented

* Corresponding author at: Berlin School of Mind and Brain, Humboldt-Universität zu Berlin, Luisenstraße 56, Haus 1, 10117 Berlin, Germany.
E-mail address: jakub.limanowski@hu-berlin.de (J. Limanowski).

1053-8119/$ – see front matter © 2013 Elsevier Inc. All rights reserved.
http://dx.doi.org/10.1016/j.neuroimage.2013.10.035

synchronously at spatially incongruent locations (palm and forearm). This synchronous stimulation countered potential problems associated with a serial, isolated presentation of observed and felt touch: For example, premotor cortex has been shown to be engaged in (serial) sensory predictions even in tasks using abstract, nonbiological stimuli (Schubotz and von Cramon, 2002, 2003, 2004), and the presentation of observed touch before felt touch at the same location could potentially be influenced by effects of anticipation of touch (see e.g. Carlsson et al., 2000; Keysers et al., 2010; Kuehn et al., 2012). Moreover, the resulting design enabled us to calculate a joint contrast comparing two RHI and control conditions, in which spatiotemporal differences between stimuli in the conditions were averaged out, and thus the resulting effects were attributable to the experienced illusion only. Second, by fully automating our experimental setup, we eliminated the human experimenter from the procedure. The induction of the RHI by touch from another person may interfere with self-related information processing, as many brain regions associated with body ownership (e.g., EBA, insula, PMv, and SI) also respond to observed human actions and touch, or mere vision of bodies of others (Bernhardt and Singer, 2012; Blanke, 2012; Ebisch et al., 2008; Keysers et al., 2010; Peelen and Downing, 2007; Zaki and Ochsner, 2012). Therefore, we aimed to isolate body ownership mechanisms from effects introduced by social interaction. The RHI has been induced automatically in one PET study (Tsakiris et al., 2007), but to our knowledge no automated MR-compatible RHI setup has been reported to date. We tested for BOLD signal differences between the RHI versus control condition within the ownership-related regions identified in previously published studies, expecting effects in regions whose response to the illusion is *not* influenced by receiving human touch. Moreover, we tested whether activity in those regions would reflect individual differences in the experienced intensity of the ownership illusion (Ehrsson et al., 2004; Petkova et al., 2011; Tsakiris et al., 2007).

Materials and methods

Participants

20 healthy volunteers (22–36 years old; 13 females; 19 right-handed, one classified as "mixed left-handed", measured with the Edinburgh Handedness Inventory, Oldfield, 1971; normal or corrected-to-normal vision) participated in the experiment; 16 of these participants took part in an additional scanning session for the functional EBA localizer. All participants gave written informed consent before the experiment and the study was approved by the local Ethical Committee of the Charité University Hospital (Berlin) and corresponded to the Human Subjects Guidelines of the Declaration of Helsinki.

Apparatus and procedure

A realistic life-size right dummy arm was mounted on a custom console made of transparent acrylic glass, which was set up atop the participant's chest (Fig. 1A). The participant's right arm was placed horizontally behind the dummy arm in a corresponding posture (distance between arms ~13 cm). To ensure that the location of visual stimuli in eye-centered coordinates remained the same, the participant was instructed to fixate a small dot in the middle of the dummy arm throughout the whole experiment, while her or his own arm was completely occluded from view (Fig. 1B). In contrast to previous studies (Ehrsson et al., 2004), our participants were not subjected to any prior information about the RHI and we collected the illusion intensity ratings after, not during the functional scanning sessions. For full, direct vision of the dummy arm, the participant's head was slightly tilted within the head coil (approx. 20–30°), her or his head and shoulders were foam-padded, the right arm was attached to the console with Velcro strips to eliminate motion during the experiment, and the gap between dummy arm and the participant's shoulder was covered with a black piece of cloth. Two pairs of sponge brushes were installed at anatomically corresponding locations at the palm and forearm of the own and dummy arms (Fig. 1B). Each of the brushes was separately moveable in back-and-forth 180° rotations, thereby applying touch at a specific location. To eliminate the influence of being touched by a human (seeing touch delivered with a hand may have specific effects on somatosensation; Ebisch et al., 2008; Keysers et al., 2010), and to ensure continuous temporal synchrony of strokes and corresponding stroking patterns, the brushes were driven by four separate electrical stepping motors placed outside the scanner room. The stepping motors (1.8° stepping angle; RS Components GmbH, Mörfelden-Walldorf, Germany) were controlled by a custom MATLAB (The MathWorks, Inc., Natick, USA) script via a computer parallel port, which also received the scanner-triggers to synchronize stimulation onsets with the fMRI acquisition. The motors' movements were mechanically transmitted to the brushes via a custom construction of nonmagnetic Plexiglas cables and plastic gears. During stimulation, the respective brushes performed strokes at 1.3 Hz, with random inter-stroke intervals (0, 50, or 150 ms), as an irregular stroking pattern has been shown to increase the RHI (Armel and Ramachandran, 2003). Before the start of the experiment, the two brushes touching the participant's own arm were adjusted and tested each, to assure reliable touch sensation. The participant then completed a brief practice run to get acquainted with the setup and the different stimulation types, and proceeded with the five experimental runs (see below). Subsequently, the strength of experienced ownership of the dummy arm in each condition was quantified (the

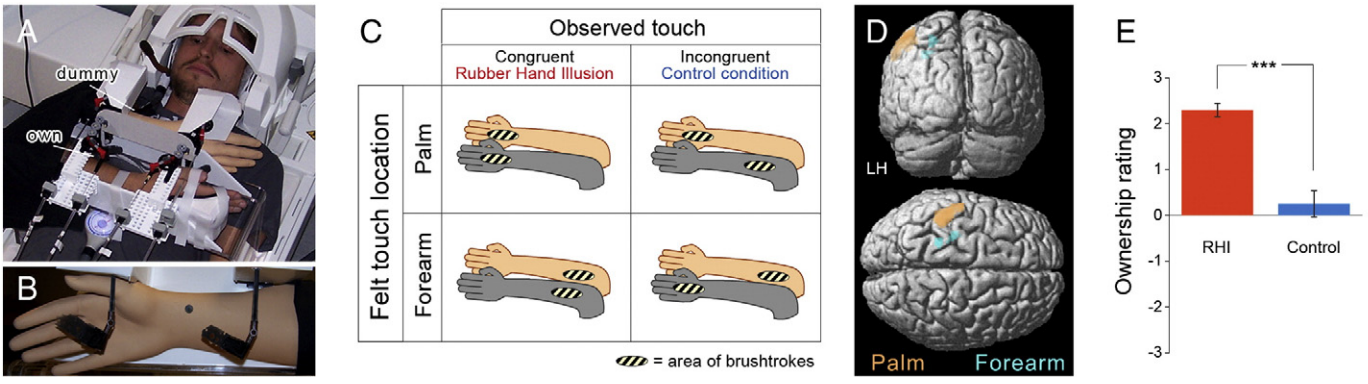

Fig. 1. (A) Experimental apparatus with the own arm occluded from view behind the dummy arm. (B) Participants' view of the dummy arm. (C) Locations of synchronous stroking on the dummy (gray) and own arm for the RHI and control condition. (D) Tactile stimulation produced significant ($p < 0.05$ FWE, small volume corrected with the left SI) activations in contralateral SI. The surface render shows the significant main effects ($p < 0.001$ uncorrected to visualize somatotopic arrangement) of stroking at the palm (x = −48, y = −38, z = 60, $t = 5.44$) and forearm (x = −24, y = −38, z = 56, $t = 3.78$) location during the visuo-tactile localizer runs, masked with anatomical left SI. (E) Participants' mean ratings of experienced ownership of the dummy arm during the RHI and control condition; error bars are standard errors of the mean, significance level obtained from Wilcoxon's signed-rank test ($z = 3.99$, $n = 20$, $p = 0.00007$).

respective two stimulation types of each condition were presented sequentially) by asking the participant to indicate her agreement with the following statement on a 7-point Likert-scale ranging from −3 ("completely disagree") to +3 ("completely agree"): "During the stimulation, it felt as if the dummy arm was my own arm." (Botvinick and Cohen, 1998). For the RHI condition the individual onset of the ownership illusion was assessed as well (Ehrsson et al., 2004): The participant was instructed to give a brief verbal response as soon as she would feel (and only if she would feel) that the dummy arm felt as if it was her own arm. The elapsed time between the beginning of stimulation and the participant's first verbal statement of experienced ownership of the dummy arm was measured with a stopwatch to represent the individual onset of the ownership illusion. After the scanning session, the participant completed a German version of the Interpersonal Reactivity Index (IRI, Davis, 1983), which has been used to measure trait empathy in other fMRI studies (e.g., Schaefer et al., 2012).

Experimental design

The scanning comprised two sessions: one for the RHI experiment and one for the functional localization of EBA and hMT+ (see below). In the first scanning session, the RHI experiment was conducted as a repeated-measures block design comprising four conditions: the RHI condition, a control condition, and a visual and tactile stroking-only condition (localizers). Each participant completed five runs, with each condition presented four times per run (presentation order of conditions was randomized for each run). Note that, due to the multi-site setup, two spatially different types of stroking could occur in each condition: The RHI condition was operationalized as synchronous stroking of anatomically corresponding locations of own and dummy arms (Botvinick and Cohen, 1998), i.e., the own and dummy arms were simultaneously either both touched at the palm, or the forearm location. In the control condition, synchronous strokes were applied to anatomically incongruent locations of own and dummy arms (i.e., simultaneous touch at the own palm and dummy forearm, or vice versa), in contrast to the typically used asynchronous stroking control condition (Armel and Ramachandran, 2003; Botvinick and Cohen, 1998; Ehrsson et al., 2004). This novel synchronous control condition was enabled by the multi-site setup; pilot experiments confirmed that, despite temporal synchrony of observed and felt touch, this condition did not induce the RHI. As functional localizers for the different visuo-tactile stimulations, we implemented a visual-only (dummy arm touch) and a tactile-only (own arm touch) condition into the design. Each stimulation was presented in a block of 17.9 s duration (18 brushstrokes), followed by a rest period of 11.2 s.

Functional localization of extrastriate body area and hMT+

In an additional scanning session, we employed a standard functional EBA localizer. This was done to functionally verify that the activation in the left middle occipital gyrus during the RHI versus control condition indeed corresponded to the location of the extrastriate body area (Downing et al., 2001). The EBA has been shown to respond more strongly to pictures of body parts versus objects (Downing and Peelen, 2011; Downing et al., 2001; Urgesi et al., 2007). Therefore, to localize EBA, participants were shown color photographs of human body parts (hands and feet), and object parts (motorcycles, following Urgesi et al., 2007) on a white background (presented on a screen viewed via a mirror at 18.7° × 13.7° visual angle). Stimulus categories were presented block-wise in random order, the order of stimuli within each block was also randomized. Fig. 3A shows sample stimuli. Each picture was presented for 700 ms followed by a 150 ms blank screen within blocks of 20 s; a black fixation cross was shown between the blocks for 20 s and served as a baseline. We calculated the contrast BODY–OBJECT to identify the effects of vision of body parts versus objects. In addition, we also localized the adjacent motion-sensitive area hMT+, because body part- (EBA) and motion-sensitive (hMT+) responses in extrastriate cortex may overlap (Spiridon et al., 2006). We used a standard motion localizer (Tootell et al., 1995): participants fixated the center of an annulus of 12° diameter, consisting of 300 randomly arranged stationary, or radially moving white dots against a black background. During motion, dots were periodically moving towards, or away from the center of the annulus (alternating every 2.25 s). Moving and stationary dots were presented with the Psychtoolbox (Brainard, 1997) alternating in blocks of 18 s length; each condition was presented 8 times. To reveal the effect of moving versus stationary stimuli, we calculated the contrast MOTION–STATIC. Sixteen participants of our RHI experiment (four were not able to participate) were scanned in this additional session. The fMRI parameters, data preprocessing, and analyses used for the functional data obtained in this scanning session were identical as described in the following for the RHI experiment.

fMRI data acquisition

The experiment was conducted on a whole-body 3 T scanner (Tim Trio, Siemens, Germany), equipped with a 32-channel head coil. T2*-weighted functional images were acquired using a customized 3D-EPI sequence (Lutti et al., 2012). Parallel imaging (GRAPPA image reconstruction) was used along the phase and partition directions (acceleration factor 2), yielding an acquisition time of 2240 ms per image volume (image resolution: 2.0 × 2.0 × 2.0 mm^3, TR = 70 ms, matrix size [96, 96, 64], TE = 33 ms, flip angle = 20°, BW = 1408 Hz). A total of 1055 functional volumes were recorded for each participant (five runs with 211 volumes each). After the functional runs and ownership ratings (see below), a high-resolution T1-weighted structural image was acquired for each participant (3D MPRAGE, voxel size = 1 mm × 1 mm × 1 mm, FOV = 256 mm × 256 mm, 176 slices, TR = 1900 ms, TE = 2.52 ms, flip angle = 9°).

Data preprocessing and analysis

Data were preprocessed and analyzed using SPM8 (Wellcome Department of Cognitive Neurology, London, UK: www.fil.ion.ucl.ac.uk/spm/). One dummy volume (38.255 s) was routinely recorded at the beginning of each run, and excluded from the analysis. Furthermore, five volumes (acquired during two rest periods) from one participant had to be discarded due to extensive movement artifacts. Individual slices of all volumes were scanned for physically-based artifacts, and, if necessary, repaired by interpolation using the SPM ArtRepair toolbox (Mazaika et al., 2009) with default settings (art_slice program; 0.08% of slices corrected). Images were then realigned to the first image of each run to correct for head motion, using a least squares approach and a 6 parameter rigid body transformation. Each participant's structural image was co-registered with the realigned functional images, and segmented into white matter, gray matter, and cerebrospinal fluid (CSF). A mask image was created from the structural CSF-segment using the SPM Volumes toolbox (thresholded to ensure 90% tissue probability), and applied to the timeseries of each run. To minimize the effect of physiological noise, the averaged timeseries of all voxels within the CSF-mask was later included into the first level design matrices as a nuisance regressor (Weissenbacher et al., 2009). Functional images were spatially normalized to the MNI standard brain (SPM8 EPI template), and spatially smoothed by an isotropic Gaussian kernel of 5 mm FWHM. Data were detrended using a linear mean global signal removal script (Macey et al., 2004). Outlier volumes showing excessive movement were identified and repaired with the SPM ArtRepair toolbox by interpolation (art_global program; default movement threshold = 0.5 mm/TR after motion correction; 2.99% of volumes repaired).

Statistical parametric maps were calculated using a standard two-level mixed-effects model. In the first-level analysis, a general linear regression model was fit to each participant's dataset. Microtime onset was set to the middle slice of each volume, and low-frequency signal

drifts in the images were removed by a high-pass filter (cut-off frequency 300 s). The six movement parameters and the extracted CSF-timeseries (see Materials and methods) were added as nuisance regressors to each run. Each stimulation type was modeled as regressors with a boxcar function and convoluted with the standard hemodynamic response function of SPM. Because of the two spatially distinct stroking types, this resulted in two regressors per condition: for the RHI ($RHI_{palm/palm}$ & $RHI_{arm/arm}$), control ($CONTROL_{palm/arm}$ & $CONTROL_{arm/palm}$), visual only ($VISUAL_{palm}$ & $VISUAL_{arm}$), and tactile only ($TACTILE_{palm}$ & $TACTILE_{arm}$) conditions. For each regressor, T-contrasts versus baseline were calculated in the GLM. The resulting contrast images of all participants were entered into flexible factorial within-subject GLMs at the second-level (random effect, group analysis), including a between-subjects factor modeling the subject constants. We tested for BOLD signal differences between the RHI and control condition (see Fig. 1C) with the factors Felt touch location (palm, forearm), and Observed touch (congruent, incongruent). For the RHI versus control comparison, we were interested in the effects of synchronous congruent (RHI condition) versus synchronous incongruent touch (control condition). We therefore combined the two stimulation types for each location in the contrast $RHI–CONTROL = (RHI_{palm/palm} + RHI_{arm/arm}) - (CONTROL_{palm/arm} + CONTROL_{arm/palm})$. Moreover, following the procedure described by Ehrsson et al. (2004), we tested for activity that was specifically related to the period before, or after illusion onset. To this end, we used each participant's individually assessed illusion onset (see below) to divide each of the first-level RHI and CONTROL regressors into a regressor modeling the pre-illusion-onset phase, and one modeling the post-illusion-onset phase. For each regressor, we then calculated a contrast comparing the period before illusion onset with the period after illusion onset (e.g., $RHI_{palm/palm[pre]} - RHI_{palm/palm[post]}$). On the second level, the resulting contrast images were entered into the same flexible factorial design as used for the RHI versus control comparison. To compare brain activity during the post-illusion versus pre-illusion phase, we calculated the inverse contrast on the second level. The effects of the functional localizers were investigated in a design with the factors Modality (tactile, visual), and Stroking location (palm, forearm).

We analyzed changes in brain connectivity of SI during the RHI versus control condition by means of psychophysiological interactions (Friston et al., 1997). To account for the fact that stroking occurred at two distinct locations, we calculated two separate PPIs, one for touch at the palm ($RHI_{palm/palm} - CONTROL_{arm/palm}$), and one for touch at the forearm ($RHI_{arm/arm} - CONTROL_{palm/arm}$). Spheres of 2 mm radius were constructed around each participant's individually thresholded peak voxel within contralateral SI (mean coordinates of seed regions for touch at the palm: $x = -44.1 \pm 6.5$, $y = -31.9 \pm 5.2$, $z = 52.4 \pm 8.6$; and touch at the forearm: $x = -32.1 \pm 5.7$, $y = -37.0 \pm 4.3$, $z = 60.1 \pm 10.3$; MEAN ± SD), and the first eigenvariate of the BOLD signal was extracted. The psychophysiological interaction terms for the RHI versus control condition were created, and included into GLMs. For each participant, the contrast images of the two PPIs were averaged using the imCalc function of SPM8 to obtain a single contrast image, which was entered into a one-sample *t*-test at the group-level. We also calculated a PPI with seed regions in the left EBA (mean coordinates of seed regions: $x = -49.8 \pm 4.4$, $y = -69.2 \pm 4.8$, $z = 4.2 \pm 3.2$; MEAN ± SD) to examine connectivity of EBA during the RHI versus control. The procedure differed from the described PPI only in that we calculated a single PPI on the joint first-level contrast $(RHI_{palm/palm} + RHI_{arm/arm}) - (CONTROL_{palm/arm} + CONTROL_{arm/palm})$. We also calculated a regression analysis on the first-level contrast images comparing the RHI versus the control condition $(RHI_{palm/palm} + RHI_{arm/arm}) - (CONTROL_{palm/arm} + CONTROL_{arm/palm})$ using the illusion scores (see below) as a covariate.

Effect sizes within clusters obtained from the second-level contrasts were calculated as percent signal change as follows: each cluster of interest, thresholded at $p < 0.001$, uncorrected, was saved as a binary image. We used the SPM rfxplot toolbox (Gläscher, 2009) to extract the parameter estimates for each participant's peak voxel within the cluster mask image. These values were averaged over participants to calculate group-level effect sizes; for correlation analyses, we used the individual parameter estimates of each subject. The anatomical mask for the left SI (BAs 3a, 3b, 1, and 2) was created with the Anatomy toolbox (Eickhoff et al., 2005). All reported coordinates correspond to the MNI space as used by SPM8. Neuroanatomical labels were derived from the SPM Anatomy toolbox where possible. For visualization of the results, the statistical maps were projected onto the SPM8 canonical single-subject T1 template, or rendered on a surface template. Based on our strong a priori assumptions (following published findings, see Introduction) for the anatomical location of regions involved in the RHI, we corrected for multiple comparisons using small volume correction based on pre-defined regions of interest (8 mm ROIs), applying a statistical threshold of $p < 0.05$ familywise error corrected (FWE). We used the following ROIs (RH = right hemisphere, LH = left hemisphere; odd MNI coordinates were approximated due to our voxel size of 2 versus typically 3 mm, e.g., for $x = 51$ we used $x = 52$): PMv (from Ehrsson et al., 2004; RH: $x = 48$, $y = 18$, $z = 40$; LH: $x = -58$, $y = 16$, $z = 10$), AI (from Ehrsson et al., 2007; RH: $x = 40$, $y = 28$, $z = 6$; LH: $x = -42$, $y = 20$, $z = 10$), PPC/IPS (from Ehrsson et al., 2004; RH: $x = 34$, $y = -46$, $z = 52$; LH: $x = -36$, $y = -42$, $z = 52$). For the EBA, we initially used the coordinates provided by Downing et al. (2001; RH: $x = 50$, $y = -70$, $z = 0$; LH: $x = -50$, $y = -72$, $z = 8$). However, as we also functionally defined the EBA in a separate localizer in our own sample, we were able to create sample-specific ROIs for the left and right EBA by binary saving the respective clusters in the left and right lateral occipital cortex that were activated ($p < 0.05$ FWE, whole-brain) by the EBA localizer. For the right TPJ, we constructed a ROI based on a transformation of the Talairach coordinates reported by Blanke et al. (2005; RH: $x = 66$, $y = -38$, $z = 18$). For all other brain regions, we report only those activations that survived a threshold of $p < 0.05$, whole-brain FWE corrected.

Behavioral data

Participants' verbal ownership ratings did not pass the Kolmogorov–Smirnov test for normality, and were therefore compared using the nonparametric Wilcoxon's signed-rank test. For the correlation analyses with brain activity differences, we calculated individual illusion scores as a compound measure reflecting both strength and prevalence of the experienced ownership illusion during the RHI condition, based on the procedure described by Ehrsson et al. (2004): each participant's difference between ownership ratings for the RHI condition and the control condition was multiplied by the duration of experienced ownership during the timeframe of stimulation in the scanning session (i.e., by subtracting the time of reported onset of the RHI from total stimulation duration). To account for the small sample size and possible effects of behavioral outliers, we used the nonparametric Spearman's rho test for the correlation analyses. All significance levels were assessed using two-tailed tests; we report only those results that survived Bonferroni correction for the number of tests performed.

Results

Behavioral results

Participants' mean reported ownership ratings for the RHI condition were significantly higher than those for the control condition (Fig. 1E; Wilcoxon's signed-rank test, $n = 20, Z = 3.99, p = 0.00007$). Moreover, the RHI condition was the only condition in which all participants affirmed experiencing ownership of the dummy arm (i.e., all ratings were positive; mean ownership rating = 2.30, SD = 0.66). On average, participants reported experiencing the illusion after 5.66 s (SD = 5.87 s),

which means that the duration of stimulation in each block (17.9 s) was long enough to evoke the RHI. Scores on the Interpersonal Reactivity Index, including the individual subscales, did neither correlate with illusion scores of the RHI, nor with brain activity differences in any of the specified regions (Pearson's correlation coefficients, all $ps > 0.05$).

The Rubber Hand Illusion versus control condition produces brain activity in extrastriate body area and anterior insula

We were interested in the specific effects of limb ownership on brain activity as induced via our RHI setup, which differed from those used in previous fMRI studies in that (i) it was fully automated and (ii) the control condition was synchronous (i.e., temporal synchrony of visual and tactile information was given). Therefore, we first tested for BOLD signal differences between the RHI and control condition, computing the contrast $(RHI_{palm/palm} + RHI_{arm/arm}) - (CONTROL_{palm/arm} + CONTROL_{arm/palm})$. Importantly, this contrast was fully matched in terms of physical stimulus properties, i.e., location and timing for the RHI and control condition. Effects of the RHI as obtained from this contrast should reveal which of the regions of interest (see Materials and methods) were responsive to the ownership illusion, even when it was induced without social interaction. Results of this random effects group analysis are shown in Fig. 2.

We observed significant ($p < 0.05$, FWE corrected, see Table 1) increases in the BOLD signal during the RHI versus control condition in the left middle occipital gyrus (mOCG), spanning into the left anterior occipital sulcus ($x = -42, y = -68, z = 8, t = 3.54$), and in the anterior insula ($x = -40, y = 16, z = 10, t = 4.16$); there also was activity in the right anterior insula ($x = 48, y = 8, z = 10, t = 3.43$, $p < 0.001$ uncorrected).

Localization of extrastriate body area

Notably, the activity in the left mOCG for the RHI versus control condition (Fig. 2) comprised coordinates of the extrastriate body area as reported by several studies (Astafiev et al., 2004; Downing et al., 2001). However, the EBA is adjacent to, and may be overlapping with the motion-sensitive region hMT+ (Peelen and Downing, 2007; Spiridon et al., 2006). We therefore ran standard functional localizers for EBA and hMT+ in 16 of the same participants in a separate scanning session (see Materials and methods), to attribute the activation in the left mOCG either to the EBA (a body part-selective region), or hMT+ (a motion-sensitive region) in our own sample.

Table 1
Group results: BOLD signal differences between the RHI versus control condition.

Anatomical location	Peak MNI ($p < 0.001$)			Peak t value
	x	y	z	
L. middle occipital gyrus	−42	−68	8	3.54[a]
L. anterior insula	−40	16	10	4.16[a]
R. anterior insula	48	8	10	3.49

Significant BOLD activations for the contrasts RHI–CONTROL.
[a] $p < 0.05$ FWE corrected based on pre-defined ROIs.

For the group-level contrast BODY–OBJECT, i.e., vision of body parts versus motorcycle parts (Fig. 3A, following Urgesi et al., 2007), we found significant ($p < 0.05$, FWE) activations in bilateral middle occipital gyrus (LH: $x = -52, y = -66, z = 6, t = 7.62$; RH: $x = 56, y = -60, z = 14, t = 6.49$), left superior parietal lobule ($x = -32, y = -44, z = 56, t = 5.52$), and left IPC/supramarginal gyrus ($x = -62, y = -28, z = 28, t = 5.46$), see Fig. 3B. Thus the EBA localizer produced strongest activity in bilateral mOCG, in agreement with published findings (Astafiev et al., 2004; Costantini et al., 2011). Next, we calculated the MOTION–STATIC contrast to locate hMT+, and found significant ($p < 0.05$, FWE) activity in the bilateral middle and inferior occipital cortex. The resulting activation in the left mOCG ($x = -42, y = -70, z = 0, t = 10.62$) was located more posterior and more inferior, and only marginally overlapped with the left EBA as defined by the BODY–OBJECT contrast (only 3 common voxels, see Fig. 3B), and not at all with the activation found for the RHI versus control condition (no common voxels, see also Fig. 2 and Table 1). Most importantly, the activation within the left mOCG as obtained from the RHI–CONTROL contrast was largely (72.7% of voxels, or 86.4% of voxels, for a mask threshold of $p < 0.05$, FWE, or $p < 0.001$, uncorrected) located within the area defined by the BODY–OBJECT contrast, and correspondingly significant at $p < 0.05$ FWE using small volume correction

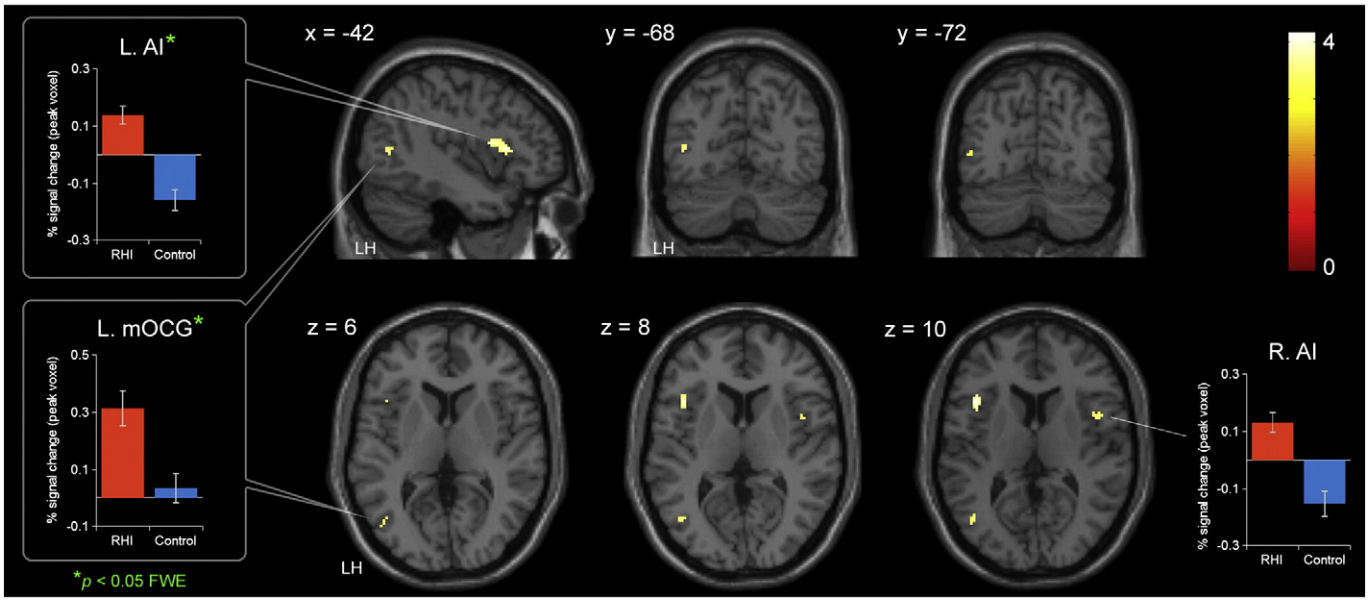

Fig. 2. Significant ($p < 0.05$ FWE correction based on pre-defined ROIs marked by a green asterisk) group-level BOLD signal differences between the Rubber Hand Illusion versus control condition $(RHI_{palm/palm} + RHI_{arm/arm}) - (CONTROL_{palm/arm} + CONTROL_{arm/palm})$. The statistical parametric maps of the T-contrast (superimposed onto the single-subject T1 template of SPM8, displayed at $p < 0.001$) show stronger activity in the left middle occipital gyrus (L. mOCG; $x = -42, y = -68, z = 8, t = 3.53$), left anterior insula (L. AI; $x = -40, y = 16, z = 10, t = 4.16$), and right anterior insula (R. AI; $x = 48, y = 8, z = 10, t = 3.49$, n.s.). The bar graphs show the mean BOLD signal changes (in percent) at peak voxels within each of these regions during the RHI and control conditions, error bars are standard errors of the mean. LH, left hemisphere.

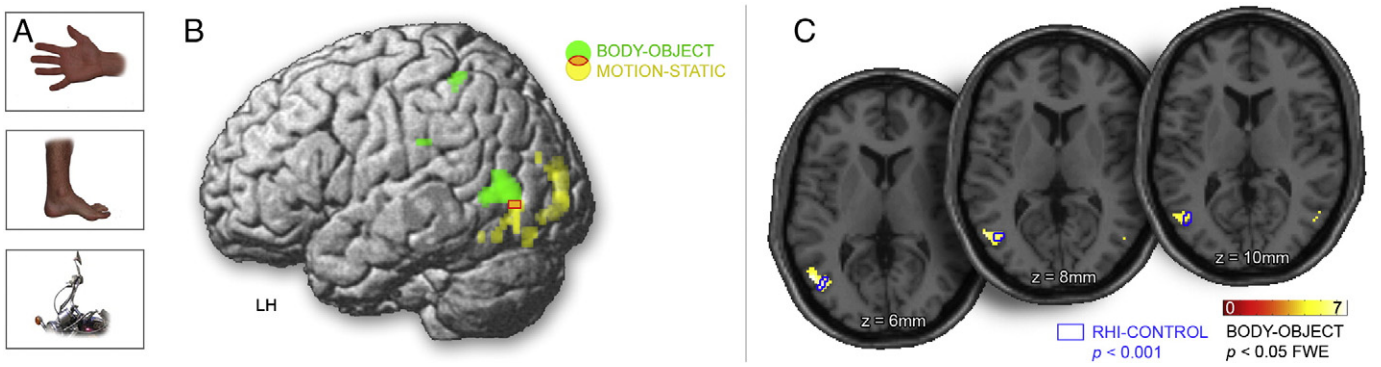

Fig. 3. (A) Sample stimuli used for locating specific responses to vision of body parts versus objects (EBA localizer). (B) Surface render of the significant ($p < 0.05$, FWE) voxels obtained from the EBA localizer (BODY–OBJECT, in green) and the MT+ localizer (MOTION–STATIC, in yellow). Overlap of these activations is indicated by a red outline (3 shared voxels). (C) Comparison of the location of activity in the left mOCG: The significant cluster in the left mOCG obtained from the BODY–OBJECT contrast ($p < 0.05$, FWE) contained 72.7% ($p < 0.05$ FWE, small volume corrected) of the significant voxels in the left mOCG as obtained from the RHI–CONTROL contrast ($p < 0.001$, uncorrected, cluster volume marked by blue outline).

with the left EBA mask (see Figs. 3B and C). Thus the functional localizer confirmed that the activity in the left mOCG for the RHI–CONTROL contrast can indeed be attributed to the left EBA, and does not overlap with the motion-sensitive area hMT+.

Activity differences in extrastriate body area correlate strongly positively with respective individual illusion scores

Our group-level comparison revealed a stronger *overall* activity of the left EBA and AI during the RHI versus control condition. However, the susceptibility to the RHI typically varies between individuals, and it is thus desirable to relate brain activity differences produced by the illusion to the observed between-subject differences in the experienced illusion. Therefore, we extracted the parameter estimates of participants' left EBA peak voxels of the RHI–CONTROL group-level contrast, selecting from within an independent ROI defined by the functional EBA localizer (Fig. 4, left) and correlated them with the respective behavioral illusion scores (a quantification of the intensity, i.e., strength

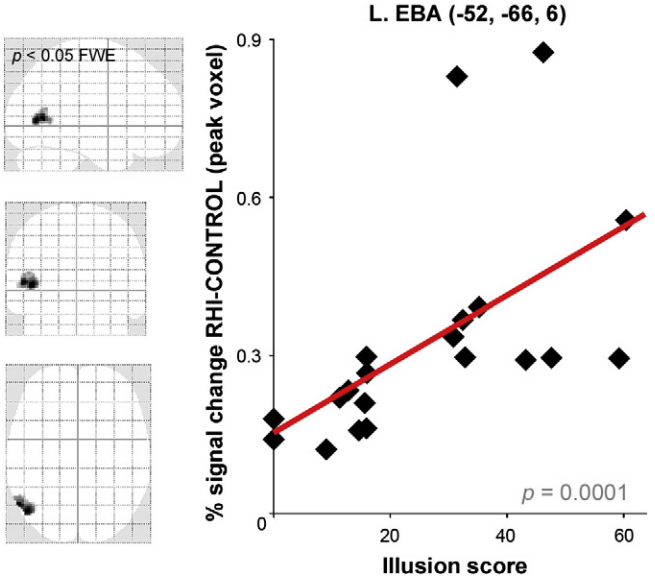

Fig. 4. Plot showing the strong positive correlation (Spearman's $\rho = 0.756$, $n = 20$, $p = 0.0001$) between BOLD signal differences at EBA peak voxels between RHI and control condition, and participants' respective illusion scores (see Materials and methods), and a least squares regression line. Peak voxels were selected from within the left EBA as localized by the BODY–OBJECT contrast in the second scanning session (see maximum intensity projection of the ROI mask, $p < 0.05$, FWE).

and prevalence of the ownership illusion during the RHI relative to the control condition, see Materials and methods). Participants' BOLD signal differences between RHI and control condition within the left EBA correlated significantly positively (Spearman's $\rho = 0.756$, $n = 20$, $p = 0.0001$) with their respective illusion scores: the higher participants scored on the illusion measure, the higher was the activity in their left EBA during the RHI versus control condition (Fig. 4, right). Activity in the left EBA thus directly reflected the subjectively experienced strength and prevalence of the ownership illusion of the dummy arm. Peak voxels within the left and right AI (regions of interest from the RHI–CONTROL group-level contrast) did not correlate significantly with illusion scores ($ps > 0.2$; the correlation of the left EBA voxels and illusion scores remained significant at $p < 0.001$ after Bonferroni correction accounting for the three tests performed). To test how specific the correlation of illusion scores in the left EBA was, we also calculated a whole-brain regression analysis on the RHI versus control contrast images, using the calculated illusion scores of our participants as a covariate. This analysis revealed that the intensity of the illusion was indeed significantly reflected only within the left EBA ($x = -52$, $y = -64$, $z = 2$, $t = 3.79$, $p < 0.05$ FWE, small volume corrected within the left EBA localizer mask) and the right PPC/IPS ($x = 18$, $y = -60$, $z = 66$, $t = 8.29$, $p < 0.05$ FWE). Importantly, only 3 of the voxels activated by this analysis were contained within the activation obtained from the hMT+ localizer (these did not survive small volume correction). This analysis thus confirmed the specificity of the relationship between EBA activity and the reported intensity of the illusion.

Stronger functional coupling among somatosensory cortex and extrastriate body area during the Rubber Hand Illusion

Activity differences between the RHI and control condition did not emerge in SI, which is not surprising due to the well-matched stimuli of the RHI and control condition (i.e., in the RHI–CONTROL contrast, tactile information was equal). However, we were interested in whether SI would still show a different connectivity pattern during the RHI versus control condition. Hence we calculated a PPI with seed regions located in the left SI (see Materials and methods). This analysis revealed that the left SI showed a significantly stronger coupling with the left ($x = -46$, $y = -72$, $z = 8$, $t = 4.98$) and right EBA ($x = 50$, $y = -66$, $z = 12$, $t = 3.99$) during the RHI versus control condition ($p < 0.05$, FWE, small volume corrected for bilateral EBA as defined by our functional localizer). Notably, the activity in the left mOCG revealed by this PPI also contained 45.5% of the voxels of the significant cluster in the left mOCG obtained from the RHI–CONTROL group-level contrast. Fig. 5 shows the location of significant voxels from this PPI analysis.

We also calculated a PPI analysis with seed regions located in the left EBA (see Materials and methods). This revealed that during the RHI

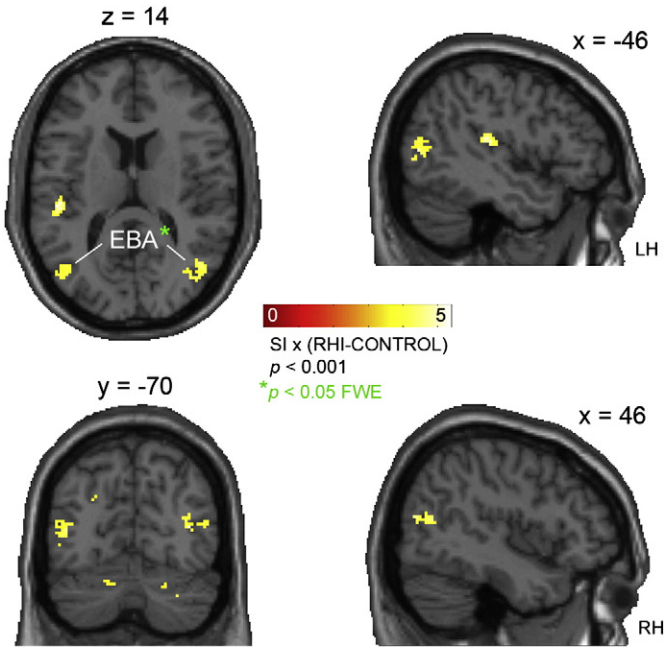

Fig. 5. Significant voxels obtained from the psychophysiological interaction analysis revealing stronger coupling of the left SI with the left (x = −46, y = −72, z = 8, $t = 4.98$, $p < 0.05$ FWE, small volume corrected) and right EBA (x = 50, y = −66, z = 12, $t = 3.99$, $p < 0.05$ FWE, small volume corrected), during the RHI versus control condition (displayed at $p < 0.001$, uncorrected).

versus control condition, the left EBA showed increased connectivity to a number of brain regions that were also activated by the EBA localizer (contrast BODY–OBJECT, thresholded at $p < 0.001$ uncorrected), namely the left supramarginal gyrus (x = −52, y = −26, z = 30, $t = 5.60$, $p < 0.05$ FWE, small volume corrected with the EBA localizer), right parietal operculum (x = 54, y = −26, z = 20, $t = 4.67$), and right anterior IPS (x = 40, y = −38, z = 50, $t = 4.27$). Although these activations partly did not survive correction for multiple comparisons, the coordinates correspond to those reported by previous related studies, which have demonstrated that these regions are involved in multisensory integration in hand-centered space (Brozzoli et al., 2011, 2012; Gentile et al., 2011; Makin et al., 2008).

Specific brain activity related to the periods before and after illusion onset

No premotor activity emerged in any of these analyses. However, in the fMRI study by Ehrsson et al. (2004), PMv activity during the RHI condition was specifically associated with the period after, relative to the period before illusion onset. We hence aimed at testing for similar interactions in our data. It should, however, be noted that in our experiment, illusion ratings were collected in the post-scanning phase, and thus these analyses have to be considered with some caution. Following the procedure described by Ehrsson et al. (2004), we first tested for activity differences between RHI and control condition during the period before participants reported the illusion, relative to the period after illusion onset. Coordinates and corrections for multiple comparisons of these activations are reported in Table 2. We replicated the findings by Ehrsson et al. (2004) during the pre-illusion period in the right dorsal premotor cortex and supplementary motor area, as well as in the left PPC/aIPS. Moreover, we found significant activations in the right TPJ (corresponding to published coordinates), left supramarginal gyrus (SMG), and bilateral EBA. Interestingly, the activations we found in EBA, PPC/aIPS, and SMG during the pre-illusion period corresponded to activations within brain regions produced by the EBA localizer (see Table 2). Next, we tested for brain activity specifically associated with the illusion period, relative to the period before onset, i.e., the inverse interaction. We found significant ($p < 0.05$ FWE) activity in the left

Table 2
Interaction: brain activity differences between RHI versus control condition before, relative to after illusion onset.

Anatomical location	Peak MNI ($p < 0.001$)			Peak t value
	x	y	z	
L. supramarginal gyrus	−46	−72	8	5.95[ac]
R. TPJ	50	−36	26	5.82[ab]
L. precuneus	−14	−66	34	5.59[a]
R. lateral occipital cortex (EBA)	52	−64	12	4.68[c]
R. dorsal premotor cortex	42	−2	58	4.46[b]
R. supplementary motor area	12	2	76	4.40[b]
L. PPC/aIPS	−28	−48	60	4.34[bc]
L. lateral occipital cortex (EBA)	−48	−72	12	4.21[c]

Stronger activity during the RHI versus control condition in the period before, relative to the period after reported illusion onset ($p < 0.05$ FWE corrected based on [a]whole-brain; [b]pre-defined ROIs; [c]EBA localizer).

paracentral lobule, spanning to the left precuneus (x = −6, y = −32, z = 80, $t = 5.90$). We also found activity in the left (x = −32, y = 20, z = 54, $t = 5.19$) and right (x = 40, y = 20, z = 56, $t = 3.67$) dorsolateral prefrontal cortex, left superior temporal gyrus (x = −44, y = −50, z = 12, $t = 5.08$) and right cerebellum (x = 32, y = −66, z = −38; $t = 5.07$), but none of these activations survived statistical correction for multiple comparisons. We did not find significant activity in PMv even when the statistical threshold was lowered to $p < 0.01$ uncorrected.

Discussion

Illusory ownership of a dummy arm was successfully induced by our novel, fully automated RHI setup, as indicated by the participants' ratings. Moreover, we found significant brain activity differences between the RHI and control condition in several of the expected brain regions. Our results, in particular the correlation of illusion scores and left EBA activity, further demonstrate a correspondence of behavioral and neural measures of illusory ownership. As we excluded the possibility that another person's presence or actions would bias participants' neural responses during stimulation, the resulting brain activity changes can be interpreted as directly underlying the illusory limb ownership, caused by congruent multisensory stimulation independent of social interaction. This is further supported by the fact that behavioral and BOLD effects of the RHI were independent of participants' trait empathy scores, which suggests that the induced ownership experience cannot be explained as a mere empathic reaction, but involves more basic mechanisms of body ownership. We will now discuss the individual findings in more detail.

Activity in extrastriate body area reflects illusory limb ownership

We found stronger brain activity in EBA during the RHI versus control condition, contralateral to the stimulated arm. ROI analyses based on published coordinates and an independent functional localizer session verified that this activation was indeed located in the body-part selective EBA. Importantly, BOLD signal responses in EBA were reflecting not only group-level differences between the RHI and the control condition, but also correlated strongly positively with interindividual differences in intensity of the RHI experience. Note also that these differences in EBA activity emerged even though a human-like arm was visible throughout the whole experiment, which alone should suffice to activate EBA.

The importance of vision for body-perception (Peelen and Downing, 2007) and specifically for the RHI (Armel and Ramachandran, 2003; Botvinick and Cohen, 1998; Pavani et al., 2000; Tsakiris and Haggard, 2005) is widely acknowledged, and has been supported by the demonstration of strong modulatory effects of vision on touch perception in peri-hand space (Làdavas et al., 2000; Lamm and Decety, 2008; Makin

et al., 2007, 2008). However, the role of visual cortex has been mainly defined as representing the dummy hand's position in space (e.g. Makin et al., 2008). Our results now provide novel evidence that EBA is directly involved in body ownership, and thus complement recent advances in understanding the functional role of the EBA: This region responds selectively to vision of bodies and body parts (Downing and Peelen, 2011; Downing et al., 2001; Pitcher et al., 2009), changes in limb position (Astafiev et al., 2004), actions with the same limb (Orlov et al., 2010), and mental imagery of embodied self-location (Arzy et al., 2006). It has moreover been suggested that the EBA integrates visual representations of the body with somatosensory information about body parts (Costantini et al., 2011; see also Apps and Tsakiris, 2013), and that it is involved in self-identification with a body (Ionta et al., 2011). However, there is an ongoing debate about the exact nature and specifically the dynamics of representations in EBA (see Downing and Peelen, 2011 for a discussion). Our results seem to suggest an at least somewhat sophisticated function of EBA, as discussed in the following.

Interactions of visuo-tactile systems during the RHI

Analyses of brain connectivity based on PPIs revealed a stronger coupling between the left SI and bilateral EBA during the RHI versus control condition, despite the well-matched stimulations in the RHI and control condition. This finding complements the results of BOLD signal differences between the RHI versus control condition, as it suggests that the EBA not only responds to the RHI, but that the somatosensory cortex also interacts more closely with this region during illusory limb ownership. It is also noteworthy that a second PPI analysis revealed that, during the RHI versus control, left EBA activity was more strongly coupled to a number of body-selective areas that have been shown to integrate multisensory information in hand-centered space (see e.g. Brozzoli et al., 2011, 2012; Gentile et al., 2011). These results support the claim that EBA is involved in integrating somatosensory with visual information about the body (Costantini et al., 2011). Together with the somatosensory system, EBA may thus be part of the often proposed "body representation" into which multisensory input must be integrated to be self-attributed (Costantini and Haggard, 2007; Kammers et al., 2006; Tsakiris, 2010; Tsakiris et al., 2007).

Recently, it has been proposed that one function of EBA could be to minimize prediction error within a hierarchical generative model of sensory input (Apps and Tsakiris, 2013; Saygin et al., 2012). These accounts follow the assumption that the brain contains hierarchical generative models that predict its sensory input (Friston, 2010; Friston and Kiebel, 2009; Hohwy, 2007). In an inversion of such a model, the driving signal is now the prediction error (the discrepancy between predicted and actual sensory input), which has to be explained away at some level of the hierarchy. This notably fits well with the classical assumption that illusory percepts emerge from Bayesian inference, i.e., an interpretation of ambiguous sensory input under a prior model (Apps and Tsakiris, 2013; Friston, 2005). During the RHI, for instance, observed and felt touch are "bound together" by these inference mechanisms (Hohwy, 2012), which explain away prediction error associated with discrepant visual, tactile, and proprioceptive input (Apps and Tsakiris, 2013; Hohwy, 2010). Although a detailed discussion of predictive coding accounts (Friston, 2010) is beyond the scope of this discussion, we would like to emphasize how well these map onto empirical data and theoretical accounts of multisensory self-processing (Blanke, 2012; Hohwy, 2007, 2010; Tsakiris, 2010; see Limanowski and Blankenburg, 2013, for a review). For our data, one potential explanation would be that indeed EBA and the interacting body-selective regions explain away prediction error that is associated with sensory input during the illusion (such as the discrepancy in visual appearance between the own and dummy arms). This would explain why activity in these regions was stronger in the period before illusion onset. In fact, a recent theoretical paper (Apps and Tsakiris, 2013) has proposed a cortical network subserving prediction error minimization during the RHI, involving the EBA at intermediate levels, and AI, rTPJ, and PMv as multimodal areas at higher levels. Interestingly, a recent study (Apps et al., 2013) found that, along with activity in multimodal rTPJ and IPS, activity in unimodal visual cortex was related to illusory self-identification with another face induced by multisensory stimulation (a paradigm similar to the RHI). Specifically, illusory ownership of a face was related to activity in the face-selective occipital face area, which nicely complements our findings of an involvement of the body-selective EBA during illusory ownership of an arm. Our results are thus in line with the findings by Apps et al. (2013) and with the claim that representations of the self are dynamically updated during these experimentally induced illusions (Apps and Tsakiris, 2013; Apps et al., 2013; Hohwy, 2012). However, as our experiment was not designed to test these theories directly, future studies will have to address whether EBA is involved in perceptual assimilation of the dummy arm during the illusion (Longo et al., 2009), and if such effects can indeed be explained within a predictive coding framework (Apps and Tsakiris, 2013; Friston, 2010; Hohwy, 2007).

It is noteworthy that activity in posterior regions, including rTPJ, left PPC/aIPS and SMG, and bilateral EBA, in addition to PMd and SMA, was stronger during the period before illusion onset. These regions are well-known to receive multimodal input (Blanke, 2012; Brozzoli et al., 2011, 2012; Gentile et al., 2011; Petkova et al., 2011; Tsakiris, 2010). Thus we partly replicated the results of Ehrsson et al. (2004), who found several of these regions to be similarly involved in the "re-calibration phase" before illusion onset, presumably by resolving inter-sensory conflict (Makin et al., 2008). The strong activation of rTPJ during this phase should be mentioned in particular, as this region has been proposed to represent and integrate information in internal models of the body (Ionta et al., 2011; Tsakiris et al., 2008). Lesions to rTPJ are associated with out-of-the-body experiences (Blanke et al., 2002, 2005), and similarly, experimentally manipulated self-location activates this region (Ionta et al., 2011).

Finally, our results suggest that several of the regions showing an early activation during the RHI are also body part-selective, as demonstrated by their activation by the EBA localizer. In this light, the reflection of illusion scores by activity in the left EBA and right PPC we found in the regression analysis is particularly interesting, as both regions were also activated by the EBA localizer. Right PPC is known to integrate spatio-temporal information and represent external reference frames (Azañón et al., 2010; Dijkerman and de Haan, 2007; Tsakiris, 2010), and has often been shown to be involved in the RHI (Evans and Blanke, 2012; Makin et al., 2008) and in self-other differentiation in general (Decety and Sommerville, 2003; Shimada et al., 2005). In conclusion, it seems that the experience of illusory hand ownership during the RHI is enabled by an early activation of a network of multimodal body-selective areas.

Anterior insula is active during the Rubber Hand Illusion

We found significant activity differences in bilateral anterior insula during the RHI versus control condition. Previous experiments have revealed an involvement of the insula in the RHI: In a PET study (Tsakiris et al., 2007), activity in the right insula reflected the mislocalization of participants' own arm during the RHI. An fMRI study (Ehrsson et al., 2007) found increased activity in bilateral AI when a dummy hand was threatened during the illusion; this threat response also correlated positively with participants' ownership ratings. While one of the main functions of AI is interoception, a more general role of AI in self-related information processing has been suggested by recent proposals. In the human insular cortex, a posterior-to-anterior increase in the complexity of representations has been suggested (Craig, 2010, 2011; Lamm and Singer, 2010), with AI involved in representations of the self, interoception, and self-awareness (Craig, 2009, 2011; Critchley et al., 2004). AI also seems to be engaged in a sense of agency (Tsakiris, 2010). A role of AI in body ownership has also been implied by the fact that individuals with an obsessive desire to amputate their limb

have a smaller cortical volume of AI, predominantly contralateral to the affected limb (Hilti et al., 2012). Crucially, AI also seems to be involved in the prediction and integration of intero- and exteroceptive information (Lamm and Singer, 2010; Singer and Lamm, 2009). Seth et al. (2011) have proposed a role of AI in a model of integrated self-representation based on interoception, "alongside models of body ownership based on proprioception and multisensory integration". The link between interoceptive and exteroceptive self-processing receives support from studies using the RHI paradigm, in which interoceptive sensibility predicted the susceptibility to the RHI (Tsakiris et al., 2011), and illusory hand or full body ownership has been shown to influence homeostatic regulation (Moseley et al., 2008; Salomon et al., 2013). Interestingly, the AI has also been suggested to be involved in conscious error processing per se (Klein et al., 2013). Correspondingly, in a recent predictive coding account of self-recognition (Apps and Tsakiris, 2013, Fig. 1), the AI is emphasized as a multimodal brain area involved in explaining away prediction error associated with the Rubber Hand Illusion. Thus, although our procedure did not include threatening the dummy arm or locating the own arm, the stronger activity we found in bilateral AI during the RHI versus control condition supports the assumed importance of AI in self-perception and body ownership.

Differences to previous findings and potential limitations

We developed a fully automated setup, using computer-controlled stroking to eliminate the human agent from the RHI induction. The somatotopic arrangement enabled us to use a combined contrast to compare brain activity in the RHI versus control condition. Moreover, our control condition allowed us to present visual and tactile stimuli simultaneously, and thus to avoid the potentially problematic serial presentation of observed and felt touch (see Introduction). Contrasting with previous findings (cf. Ehrsson et al., 2004, 2005; Petkova et al., 2011), we failed to replicate effects of the illusion in ventral premotor cortex. It should be emphasized that these results have to be considered with caution, as our participants rated the strength and onset of the illusion off-line, i.e., after the scanning session (cf. Ehrsson et al., 2004). However, post-scanning ratings have been employed elsewhere (Petkova et al., 2011), and as our rating session followed immediately after the last scanning run, and participants lay in the scanner exactly as during the image acquisition, the ratings should still reflect the experienced illusion to a sufficient degree. Interestingly, a PET study (Tsakiris et al., 2007) that also used an automated setup to induce the RHI also found no PMv activity during the RHI. Similarly, a recent study using fully automated multisensory stimulation to induce illusory self-identification with another face also failed to replicate any involvement of PMv in the ownership illusion (Apps et al., 2013). This suggests that PMv activity could reflect another human agent touching one's own body—thus it would still be a measure of the illusion (and not as prominent in the control condition), albeit an indirect one. Another possible explanation for the different findings could be that premotor activity might be enabled by non-motor functions of the premotor cortex like attentional control or working memory (Schubotz et al., 2010; see Schubotz and von Cramon, 2003, for a detailed review). Premotor activity has been associated with "prospective attention to sensory events", i.e., sensory predictions (Schubotz and von Cramon, 2002, 2003) even for abstract, non-biological stimuli (Schubotz and von Cramon, 2004). It could thus be that PMv activity did not emerge in our study because stimulations in both RHI and control condition were synchronous, and thus did not differ in terms of temporal attentional demands. However, we did not directly contrast the automated induction of the RHI with an induction performed by a human experimenter, or spatially incongruent with temporally asynchronous stroking, and therefore our explanation remains speculative.

While our design eliminated differences in temporal attentional demands between RHI and control condition, it could be argued that these now differed in terms of crossmodal spatial attention. Crossmodal spatial and temporal attention seems to play an important role in tasks involving visuo-tactile interactions (Macaluso and Driver, 2001; Pavani et al., 2000; Spence et al., 2000). However, as noted recently by Macaluso and Maravita (2010), the effects of visuo-tactile interactions in peripersonal space "do not appear to be merely related to spatial attention control" and "can trigger specialized processes associated with embodiment and sense of body ownership." Also, one would not expect such a specific effect as we found in the left EBA (contralateral to the stimulated arm), because by the calculation of the joint contrast of both RHI and both control conditions, differences between them was averaged out. Finally, it should also be mentioned that the body- and motion-selective responses we found in lateral occipital cortex overlapped in some analyses. However, the effects of the illusory experience were specific to the body-selective regions as defined by the EBA localizer.

Conclusion

Using a novel, fully automated fMRI setup, we induced illusory limb ownership in healthy participants, isolated from social interaction. Thereby we have demonstrated for the first time that the extrastriate body area (EBA) not only shows a preference for seeing body parts (which we replicated using a functional localizer), but particularly when those are also experienced as part of one's own body. This interpretation is supported by the fact that (i) EBA activity is significantly stronger during the RHI versus control condition, (ii) activity differences between RHI and control condition in the left EBA correlate strongly positively with participants' respective behavioral illusion scores, and (iii) SI contralateral to the stimulated arm is more strongly coupled with bilateral EBA during the RHI versus control condition. Our results thus provide novel evidence for dynamic representations in EBA, and show that the RHI paradigm can be used to gain further insight into the functional role of the EBA.

Acknowledgments

This research was supported by a grant from the German Federal Ministry of Education and Research (BMBF) to FB. We thank R. Auksztulewicz, and B. Spitzer for comments, and E. Kirilina for technical advice. The authors declare no competing financial interests.

References

Apps, M.A., Tsakiris, M., 2013. The free-energy self: a predictive coding account of self-recognition. Neurosci. Biobehav. Rev. http://dx.doi.org/10.1016/j.neubiorev.2013.01.029 (Epub ahead of print).

Apps, M.A., Tajadura-Jiménez, A., Sereno, M., Blanke, O., Tsakiris, M., 2013. Plasticity in unimodal and multimodal brain areas reflects multisensory changes in self-face identification. Cereb. Cortex. http://dx.doi.org/10.1093/cercor/bht199 (Epub ahead of print).

Armel, K.C., Ramachandran, V.S., 2003. Projecting sensations to external objects: evidence from skin conductance response. Proc. Biol. Sci. 270, 1499–1506.

Arzy, S., Thut, G., Mohr, C., Michel, C.M., Blanke, O., 2006. Neural basis of embodiment: distinct contributions of temporoparietal junction and extrastriate body area. J. Neurosci. 26, 8074–8081.

Astafiev, S.V., Stanley, C.M., Shulman, G.L., Corbetta, M., 2004. Extrastriate body area in human occipital cortex responds to the performance of motor actions. Nat. Neurosci. 7, 542–548.

Azañón, E., Longo, M.R., Soto-Faraco, S., Haggard, P., 2010. The posterior parietal cortex remaps touch into external space. Curr. Biol. 20, 1304–1309.

Bernhardt, B.C., Singer, T., 2012. The neural basis of empathy. Ann. Rev. Neurosci. 35, 1–23.

Blanke, O., 2012. Multisensory brain mechanisms of bodily self-consciousness. Nat. Rev. Neurosci. 13, 556–571.

Blanke, O., Metzinger, T., 2009. Full-body illusions and minimal phenomenal selfhood. Trends Cogn. Sci. 13, 7–13.

Blanke, O., Mohr, C., 2005. Out-of-body experience heautoscopy and autoscopic hallucination of neurological origin Implications for neurocognitive mechanisms of corporeal awareness and self-consciousness. Brain Res. Rev. 50, 184–199.

Blanke, O., Ortigue, S., Landis, T., Seeck, M., 2002. Stimulating illusory own-body perceptions. Nature 419, 269–270.

Blanke, O., Mohr, C., Michel, C.M., Pascual-Leone, A., Brugger, P., Seeck, M., Landis, T., et al., 2005. Linking out-of-body experience and self processing to mental own-body imagery at the temporoparietal junction. J. Neurosci. 25, 550–557.
Botvinick, M., Cohen, J., 1998. Rubber hands "feel" touch that eyes see. Nature 391, 756.
Brainard, D.H., 1997. The Psychophysics Toolbox. Spat. Vis. 10, 433–436.
Brozzoli, C., Gentile, G., Petkova, V.I., Ehrsson, H.H., 2011. FMRI adaptation reveals a cortical mechanism for the coding of space near the hand. J. Neurosci. 31, 9023–9031.
Brozzoli, C., Gentile, G., Ehrsson, H.H., 2012. That's near my hand! Parietal and premotor coding of hand-centered space contributes to localization and self-attribution of the hand. J. Neurosci. 32, 14573–14582.
Carlsson, K., Petrovic, P., Skare, S., Peterson, K.M., Ingvar, M., 2000. Tickling expectations: neural processing in anticipation of a sensory stimulus. J. Cogn. Neurosci. 12, 691–703.
Costantini, M., Haggard, P., 2007. The Rubber Hand Illusion: sensitivity and reference frame for body ownership. Conscious. Cogn. 16, 229–240.
Costantini, M., Urgesi, C., Galati, G., Romani, G.L., Aglioti, S.M., 2011. Haptic perception and body representation in lateral and medial occipito-temporal cortices. Neuropsychologia 49, 821–829.
Craig, A.D.B., 2009. How do you feel-now? The anterior insula and human awareness. Nat. Rev. Neurosci. 10, 59–70.
Craig, A.D.B., 2010. The sentient self. Brain Struct. Funct. 214, 563–577.
Craig, A.D.B., 2011. Significance of the insula for the evolution of human awareness of feelings from the body. Ann. N. Y. Acad. Sci. 1225, 72–82.
Critchley, H.D., Wiens, S., Rotshtein, P., Ohman, A., Dolan, R.J., 2004. Neural systems supporting interoceptive awareness. Nat. Neurosci. 7, 189–195.
Davis, M.H., 1983. Measuring individual differences in empathy: evidence for a multidimensional approach. J. Pers. Soc. Psychol. 44, 113–126.
Decety, J., Sommerville, J.A., 2003. Shared representations between self and other: a social cognitive neuroscience view. Trends Cogn. Sci. 7, 527–533.
Dijkerman, H.C., de Haan, E.H.F., 2007. Somatosensory processes subserving perception and action. Behav. Brain Sci. 30, 189–239.
Downing, P.E., Peelen, M.V., 2011. The role of occipitotemporal body-selective regions in person perception. Cogn. Neurosci. 2, 37–41.
Downing, P.E., Jiang, Y., Shuman, M., Kanwisher, N., 2001. A cortical area selective for visual processing of the human body. Science 293, 2470–2473.
Ebisch, S.J.H., Perrucci, M.G., Ferretti, A., Del Gratta, C., Romani, G.L., Gallese, V., 2008. The sense of touch: embodied simulation in a visuotactile mirroring mechanism for observed animate or inanimate touch. J. Cogn. Neurosci. 20, 1611–1623.
Ehrsson, H.H., 2007. The experimental induction of out-of-body experiences. Science 317, 1048.
Ehrsson, H.H., Spence, C., Passingham, R.E., 2004. That's my hand! Activity in premotor cortex reflects feeling of ownership of a limb. Science 305, 875–877.
Ehrsson, H.H., Holmes, N.P., Passingham, R.E., 2005. Touching a rubber hand: feeling of body ownership is associated with activity in multisensory brain areas. J. Neurosci. 25, 10564–10573.
Ehrsson, H.H., Wiech, K., Weiskopf, N., Dolan, R.J., Passingham, R.E., 2007. Threatening a rubber hand that you feel is yours elicits a cortical anxiety response. PNAS 104, 9828–9833.
Eickhoff, S.B., Stephan, K.E., Mohlberg, H., Grefkes, C., Fink, G.R., Amunts, K., Zilles, K., 2005. A new SPM toolbox for combining probabilistic cytoarchitectonic maps and functional imaging data. NeuroImage 25, 1325–1335.
Evans, N., Blanke, O., 2012. Shared electrophysiology mechanisms of body ownership and motor imagery. NeuroImage 64, 216–228.
Friston, K., 2005. A theory of cortical responses. Philos. Trans. R. Soc. Lond. B Biol. Sci. 360, 815–836. http://dx.doi.org/10.1098/rstb.2005.1622.
Friston, K., 2010. The free-energy principle: a unified brain theory? Nat. Rev. Neurosci. 11, 127–138.
Friston, K., Kiebel, S., 2009. Predictive coding under the free-energy principle. Philos. Trans. R. Soc. B-Biol. Sci. 364, 1211–1221. http://dx.doi.org/10.1098/rstb.2008.0300.
Friston, K.J., Buechel, C., Fink, G.R., Morris, J., Rolls, E., Dolan, R.J., 1997. Psychophysiological and modulatory interactions in neuroimaging. NeuroImage 6, 218–229.
Gallagher, S., 2000. Philosophical conceptions of the self: implications for cognitive science. Trends Cogn. Sci. 4, 14–21.
Gentile, G., Petkova, V.I., Ehrsson, H.H., 2011. Integration of visual and tactile signals from the hand in the human brain: an FMRI study. J. Neurophysiol. 105, 910–922.
Gläscher, J., 2009. Visualization of group inference data in functional neuroimaging. Neuroinformatics 7, 73–82.
Hilti, L.M., Hänggi, J., Vitacco, D.A., Kraemer, B., Palla, A., Luechinger, R., Jäncke, L., et al., 2012. The desire for healthy limb amputation: structural brain correlates and clinical features of xenomelia. Brain 136, 318–329.
Hohwy, J., 2007. The sense of self in the phenomenology of agency and perception. Psyche 13, 1–20.
Hohwy, J., 2010. The hypothesis testing brain: some philosophical applications. ASCS09: Proceedings of the 9th Conference of the Australasian Society for Cognitive Science, pp. 135–144.
Hohwy, J., 2012. Attention and conscious perception in the hypothesis testing brain. Front. Psychol. 3, 96. http://dx.doi.org/10.3389/fpsyg.2012.00096.
Holmes, N.P., Spence, C., 2004. The body schema and multisensory representation(s) of peripersonal space. Cogn. Process. 5, 94–105.
Ionta, S., Heydrich, L., Lenggenhager, B., Mouthon, M., Fornari, E., Chapuis, D., Gassert, R., et al., 2011. Multisensory mechanisms in temporo-parietal cortex support self-location and first-person perspective. Neuron 70, 363–374.
Jeannerod, M., 2007. Being oneself. J. Physiol. Paris 101, 161–168.
Kammers, M.P.M., Van der Ham, I.J.M., Dijkerman, H.C., 2006. Dissociating body representations in healthy individuals: differential effects of a kinaesthetic illusion on perception and action. Neuropsychologia 44, 2430–2436.
Kanayama, N., Sato, A., Ohira, H., 2007. Crossmodal effect with Rubber Hand Illusion and gamma-band activity. Psychophysiology 44, 392–402.
Kanayama, N., Sato, A., Ohira, H., 2009. The role of gamma band oscillations and synchrony on Rubber Hand Illusion and crossmodal integration. Brain Cogn. 69, 19–29.
Keysers, C., Kaas, J.H., Gazzola, V., 2010. Somatosensation in social perception. Nat. Rev. Neurosci. 11, 417–428.
Klein, T.A., Ullsperger, M., Danielmeier, C., 2013. Error awareness and the insula: links to neurological and psychiatric diseases. Front. Hum. Neurosci. 7, 14. http://dx.doi.org/10.3389/fnhum.2013.00014.
Kuehn, E., Trampel, R., Mueller, K., Turner, R., Schütz-Bosbach, S., 2012. Judging roughness by sight-A 7-Tesla fMRI study on responsivity of the primary somatosensory cortex during observed touch of self and others. Hum. Brain Mapp. 34, 1882–1895. http://dx.doi.org/10.1002/hbm.22031.
Làdavas, E., Farnè, A., Zeloni, G., Di Pellegrino, G., 2000. Seeing or not seeing where your hands are. Exp. Brain Res. 131, 458–467.
Lamm, C., Decety, J., 2008. Is the extrastriate body area (EBA) sensitive to the perception of pain in others? Cereb. Cortex 18, 2369–2373.
Lamm, C., Singer, T., 2010. The role of anterior insular cortex in social emotions. Brain Struct. Funct. 214, 579–591.
Lenggenhager, B., Tadi, T., Metzinger, T., Blanke, O., 2007. Video ergo sum: manipulating bodily self-consciousness. Science 317, 1096–1099.
Lenggenhager, B., Halje, P., Blanke, O., 2011. Alpha band oscillations correlate with illusory self-location induced by virtual reality. Eur. J. Neurosci. 33, 1935–1943.
Limanowski, J., Blankenburg, F., 2013. Minimal self-models and the free energy principle. Front. Hum. Neurosci. 7, 547. http://dx.doi.org/10.3389/fnhum.2013.00547.
Longo, M.R., Schüür, F., Kammers, M.P.M., Tsakiris, M., Haggard, P., 2009. Self awareness and the body image. Acta Psychol. 132, 166–172.
Lutti, A., Thomas, D.L., Hutton, C., Weiskopf, N., 2012. High-resolution functional MRI at 3 T: 3D/2D echo-planar imaging with optimized physiological noise correction. Magn. Reson. Med. 69, 1657–1664. http://dx.doi.org/10.1002/mrm.24398.
Macaluso, E., Driver, J., 2001. Spatial attention and crossmodal interactions between vision and touch. Neuropsychologia 39, 1304–1316.
Macaluso, E., Maravita, A., 2010. The representation of space near the body through touch and vision. Neuropsychologia 48, 782–795.
Macey, P.M., Macey, K.E., Kumar, R., Harper, R.M., 2004. A method for removal of global effects from fMRI time series. NeuroImage 22, 360–366.
Makin, T.R., Holmes, N.P., Zohary, E., 2007. Is that near my hand? Multisensory representation of peripersonal space in human intraparietal sulcus. J. Neurosci. 27, 731–740.
Makin, T.R., Holmes, N.P., Ehrsson, H.H., 2008. On the other hand: dummy hands and peripersonal space. Behav. Brain Res. 191, 1–10.
Mazaika, P., Hoeft, F., Glover, G.H., Reiss, A.L., 2009. Methods and software for fMRI analysis for clinical subjects. Paper Presented at the Annual Meeting of the Organization for Human Brain Mapping.
Moseley, G.L., Olthof, N., Venema, A., Don, S., Wijers, M., Gallace, A., Spence, C., 2008. Psychologically induced cooling of a specific body part caused by the illusory ownership of an artificial counterpart. PNAS 105, 13169–13173.
Oldfield, R.C., 1971. The assessment and analysis of handedness: the Edinburgh inventory. Neuropsychologia 9, 97–113.
Orlov, T., Makin, T., Zohary, E., 2010. Topographic representation of the human body in the occipitotemporal cortex. Neuron 68, 586–600.
Pavani, F., Spence, C., Driver, J., 2000. Visual capture of touch: out-of-the-body experiences with rubber gloves. Psychol. Sci. 11, 353–359.
Peelen, M.V., Downing, P.E., 2007. The neural basis of visual body perception. Nat. Rev. Neurosci. 8, 636–648.
Petkova, V.I., Björnsdotter, M., Gentile, G., Jonsson, T., Li, T.Q., Ehrsson, H.H., 2011. From part- to whole-body ownership in the multisensory brain. Curr. Biol. 21, 1118–1122.
Pitcher, D., Charles, L., Devlin, J.T., Walsh, V., Duchaine, B., 2009. Triple dissociation of faces bodies and objects in extrastriate cortex. Curr. Biol. 19, 319–324.
Salomon, R., Lim, M., Pfeiffer, C., Gassert, R., Blanke, O., 2013. Full body illusion is associated with widespread skin temperature reduction. Front. Behav. Neurosci. 7, 65. http://dx.doi.org/10.3389/fnbeh.2013.00065.
Saygin, A.P., Chaminade, T., Ishiguro, H., Driver, J., Frith, C., 2012. The thing that should not be: predictive coding and the uncanny valley in perceiving human and humanoid robot actions. Soc. Cogn. Affect. Neurosci. 7, 413–422.
Schaefer, M., Heinze, H.-J., Rotte, M., 2012. Embodied empathy for tactile events: interindividual differences and vicarious somatosensory responses during touch observation. NeuroImage 60, 952–957.
Schubotz, R.I., von Cramon, D.Y., 2002. A blueprint for target motion: fMRI reveals perceived sequential complexity to modulate premotor cortex. NeuroImage 16, 920–935.
Schubotz, R.I., von Cramon, D.Y., 2003. Functional–anatomical concepts of human premotor cortex: evidence from fMRI and PET studies. NeuroImage 20, S120–S131.
Schubotz, R.I., von Cramon, D.Y., 2004. Sequences of abstract nonbiological stimuli share ventral premotor cortex with action observation and imagery. J. Neurosci. 24, 5467–5474.
Schubotz, R.I., Anwander, A., Knösche, T.R., von Cramon, D.Y., Tittgemeyer, M., 2010. Anatomical and functional parcellation of the human lateral premotor cortex. NeuroImage 50, 396–408.
Seth, A.K., Suzuki, K., Critchley, H.D., 2011. An interoceptive predictive coding model of conscious presence. Front. Psychol. 2, 395.
Shimada, S., Hiraki, K., Oda, I., 2005. The parietal role in the sense of self-ownership with temporal discrepancy between visual and proprioceptive feedbacks. NeuroImage 24, 1225–1232.
Singer, T., Lamm, C., 2009. The social neuroscience of empathy. Ann. N. Y. Acad. Sci. 1156, 81–96.
Spence, C., Pavani, F., Driver, J., 2000. Crossmodal links between vision and touch in covert endogenous spatial attention. J. Exp. Psychol. Hum. Percept. Perform. 26, 1298.

Spiridon, M., Fischl, B., Kanwisher, N., 2006. Location and spatial profile of category-specific regions in human extrastriate cortex. Hum. Brain Mapp. 27, 77–89.
Tootell, R.B., Reppas, J.B., Kwong, K.K., Malach, R., Born, R.T., Brady, T.J., Rosen, B.R., et al., 1995. Functional analysis of human MT and related visual cortical areas using magnetic resonance imaging. J. Neurosci. 15, 3215–3230.
Tsakiris, M., 2010. My body in the brain: a neurocognitive model of body-ownership. Neuropsychologia 48, 703–712.
Tsakiris, M., Haggard, P., 2005. The Rubber Hand Illusion revisited: visuotactile integration and self-attribution. J. Exp. Psychol. Hum. Percept. Perform. 31, 80–91.
Tsakiris, M., Hesse, M.D., Boy, C., Haggard, P., Fink, G.R., 2007. Neural signatures of body ownership: a sensory network for bodily self-consciousness. Cereb. Cortex 17, 2235–2244.
Tsakiris, M., Costantini, M., Haggard, P., 2008. The role of the right temporo-parietal junction in maintaining a coherent sense of one's body. Neuropsychologia 46, 3014–3018.
Tsakiris, M., Tajadura-Jiménez, A., Costantini, M., 2011. Just a heartbeat away from one's body: interoceptive sensitivity predicts malleability of body-representations. Proc. R. Soc. B-Biol. Sci. 278, 2470–2476.
Urgesi, C., Candidi, M., Ionta, S., Aglioti, S.M., 2007. Representation of body identity and body actions in extrastriate body area and ventral premotor cortex. Nat. Neurosci. 10, 30–31.
Weissenbacher, A., Kasess, C., Gerstl, F., Lanzenberger, R., Moser, E., Windischberger, C., 2009. Correlations and anticorrelations in resting-state functional connectivity MRI: a quantitative comparison of preprocessing strategies. NeuroImage 47, 1408–1416.
Zaki, J., Ochsner, K., 2012. The neuroscience of empathy: progress pitfalls and promise. Nat. Neurosci. 15, 675–680.